In-Situ X-Ray Observations of Ultrasound-Induced Explosive Decomposition

Jesus O. Mares, Jr.[1], Zane A. Roberts[2], I. Emre Gunduz[2], Niranjan D. Parab[1], Tao Sun[3], Kamel Fezzaa[3], Weinong W. Chen[1,2,4], Steven. F. Son[1,2], and Jeffrey F. Rhoads[2,*]
[1]School of Aeronautics and Astronautics, Purdue University, West Lafayette, Indiana 47907, USA
[2]School of Mechanical Engineering, Purdue University, West Lafayette, Indiana 47907, USA
[3]Advanced Photon Source, Argonne National Laboratory, Lemont, Illinois 60439, USA
[4]School of Materials Engineering, Purdue University, West Lafayette, Indiana 47907, USA
*Corresponding author. Email address: jfrhoads@purdue.edu

Abstract

High-strain mechanical loading of polymer-bonded explosives can produce significant stress concentrations due to microstructural heterogeneities, resulting in localized thermal "hot spots". Ultrasound produces similar effects and has been proposed as a tool to study the thermomechanical interactions related to explosive initiation. Detailed observations of the processes governing the generation of heat in these materials are severely lacking, yet they are vital for identifying salient physics, improving the modeling tools used to predict mechanical response, improving explosives safety, and providing insight into the initiation mechanisms of explosion. Here we report on high-speed, high-resolution *in-situ* observations, obtained via synchrotron X-ray phase contrast imaging and diffraction, of the heating and decomposition of an explosive material under ultrasonic excitation. We demonstrate that interfacial friction is a dominant heating mechanism and can yield violent reaction of explosive particles. Furthermore, sub-surface particle temperatures are estimated via diffraction.

Keywords

Hot spot, ultrasound, explosive decomposition, polymer-bonded explosive, X-ray phase contrast imaging, diffraction

1. Introduction

Recent studies have demonstrated that significant heating and even partial decomposition of composite explosive systems can be achieved through high-frequency mechanical excitation [1-7]. The capability to generate localized heating within these materials via a tunable mechanical insult may increase the understanding of thermomechanical interactions within composite explosive systems [2, 5, 8], which may prove useful in the detection of explosives. Using this phenomenon to purposefully heat a targeted explosive system and subsequently increase the detectable vapor pressure of the energetic material would greatly enhance the probability of successful identification via current detection methods [9-11]. The exploitation of this heating phenomenon may also allow for the development of novel methods suitable for the intentional defeat of a targeted explosive [12]. Additionally, the demonstrated ability of certain composite explosives to partially decompose in response to high-frequency mechanical excitation may present safety concerns for these materials when subjected to highly dynamic

environments [13, 14]. In order to fully utilize this potential capability to enhance detection and defeat, and to improve upon the safety of composite explosive systems used in unique and harsh environments, the specific mechanisms of heat generation governing this phenomenon must be better understood.

In prior work, it has been demonstrated that ultrasonic excitation can be used to drive individual energetic particles of cyclotetramethylene-tetranitramine (HMX) and ammonium perchlorate (AP) embedded within a viscoelastic binder material to decomposition [3, 6, 7]. Furthermore, these studies have shown that relatively weak mechanical energy can be concentrated and thermally dissipated at these energetic inclusions, resulting in locations of significant heating, or "hot spots". While the exact processes governing this heat generation remain unclear, various mechanisms have been suggested in prior work [3-6], including particle-particle interactions, localized viscoelastic heating due to wave interactions, friction along the particle-binder interface, and plastic deformation of the binder material. However, direct observations of these hypothesized mechanisms or the detailed decomposition of the embedded energetic particles in response to high-frequency mechanical excitation are yet to be made. Improved methods to dynamically visualize the response of these materials *in situ* in simplified configurations is needed.

The study of these energy dissipation mechanisms via ultrasonic stimulation may also extend the knowledge of "hot spot" formation within these materials in the context of explosives safety and initiation [2, 13]. These mechanisms have been suggested, in part, to lead to violent reaction and even the initiation of a detonation event within composite explosives in response to mechanical loading or shock [8, 15]. The utilization of ultrasonic excitation allows for the mechanical loading of these materials at tailored strain rates, which provides a valuable tool to investigate the response of these materials under a wide range of loading conditions. A specific investigation of the generation and progression of ultrasonically induced hot spots within these materials, as well as the specific heat generation mechanisms associated with this phenomenon, is needed.

The objective of this work is to develop a more complete understanding of the mechanisms which generate hot spots through the use of *in-situ* high-speed X-ray phase contrast imaging (HS-XPCI) and X-ray diffraction (HS-XRD) on explosive particles embedded within a binder under sustained high-frequency mechanical excitation using synchrotron radiation at the Advanced Photon Source (APS) at Argonne National Laboratory (ANL). Detailed observations were made of the physical changes, the decomposition, and the thermal expansion of individual and multiple explosive particles. Furthermore, dynamic interactions at the particle-binder interface induced via the applied ultrasound were also observed. The thermal expansion of a crystalline material causes shifts in the x-ray diffraction pattern due to the change in lattice spacing and this effect has been used in the past to measure the thermal expansion coefficient of various materials including HMX crystals [16]. Accordingly, the measured diffraction pattern shifts dynamically observed for one sample were used to infer the crystal temperature under the applied insult.

2. Material and Methods

2.1 Sample Preparation

Samples were fabricated by fully embedding HMX particles within a rectangular block of Sylgard 184, a visibly transparent binder material. All of the Sylgard 184 material used in this study was doped with 0.01% by mass of iron oxide particles (nominally 44 μm) in order to increase the contrast between the binder and HMX for the purpose of the X-ray imaging. The samples were constructed by casting an initial layer of 10:1 base to curative mixture of Sylgard 184 in a flat dish to a height of approximately 1 mm. The layer was cured at 65 °C for a minimum of 12 hrs and an additional layer of Sylgard 184 was then poured onto the cured layer to a total height of approximately 4 mm. For the single particle samples, one HMX particle was placed within the uncured Sylgard 184 layer and allowed to settle to the surface of the bottom cured layer. A similar process was used for the multiple particle samples, where a small amount of HMX was scattered across the sample into the uncured layer. All of the HMX particles used in this study were selected from a lot of grade B class 3 HMX particles sieved to +30 mesh (500 μm). Samples measuring approximately 6.6 x 9.0 x 4.0 mm were cut from the layered binder particle system. Single particle samples were cut such that the HMX particle was centered within the sample.

2.2 Mechanical Excitation

Steiner & Martins, Inc. SMD10T2R111 lead zirconate titanate (PZT) ultrasonic piezoelectric transducers were used to apply high-frequency mechanical excitation to each sample. The transducer was specified to operate in a radial mode at the listed center frequency of 215 kHz ±3%. A single transducer was epoxied to the bottom side of each sample with Devcon 5-minute epoxy and cured at 65 °C for a minimum of 12 hrs. A sinusoidal electrical signal was delivered to the ultrasonic transducers via an Agilent N9310A RF signal generator in concert with a Mini-Circuits LZY-22+ broadband amplifier. A Tektronix DPO 4043 oscilloscope was used to monitor the supply signal delivered to the transducer. For all of the trials reported in this work, a continuous electrical signal of 210 kHz was supplied to the transducer at a power of 10 W.

2.3 High-Speed X-Ray Phase Contrast Imaging and Diffraction

High-speed X-ray phase contrast imaging was used to observe the highly dynamic behavior of the energetic particle within the viscoelastic binder material under high-frequency mechanical excitation. For the results presented in this study, polychromatic (white beam), high intensity X-ray phase contrast imaging was performed at beam line 32-ID-B at the Advanced Photon Source (APS) at Argonne National Laboratory. The 1st harmonic energy of the X-ray source used for imaging had a peak at 24.2 keV with an undulator gap of 12 mm (Fig. 1), and the size of the beam on sample was 2560 x 1500 μm^2. To visualize the X-ray information, a single crystal $Lu_3Al_5O_{12}$:Ce scintillator was used to transform the X-ray signal to visible wavelength light.

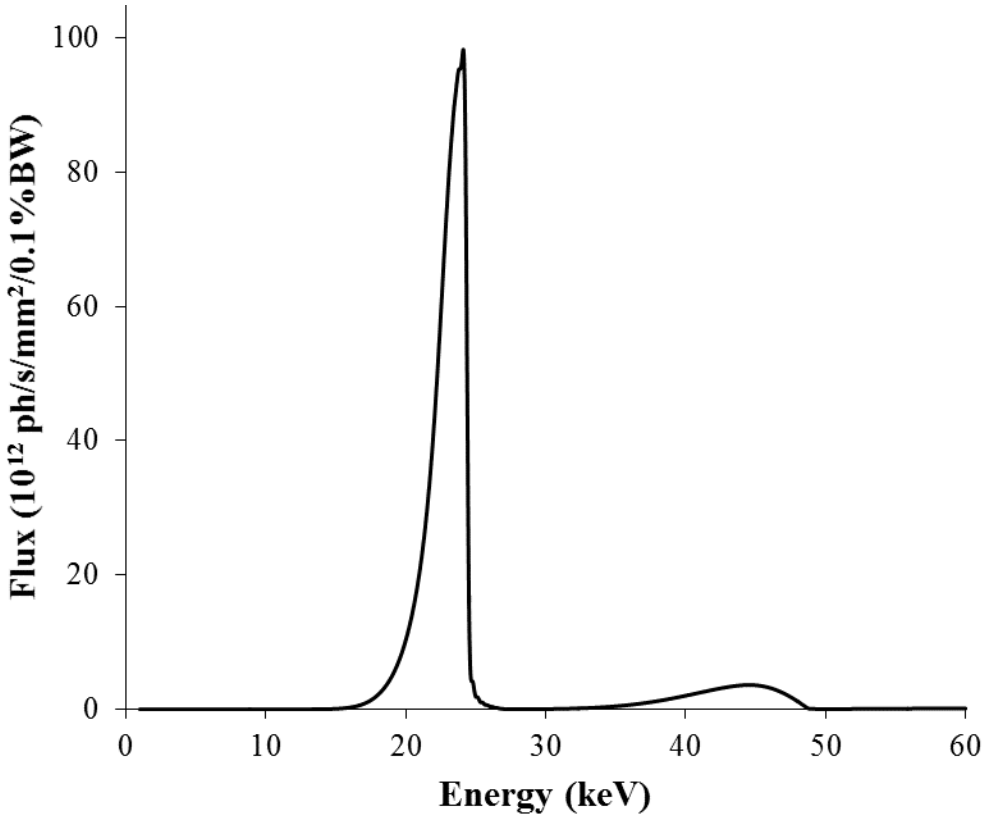

Figure 1. White-beam X-ray energy spectrum with an undulator gap of 12 mm.

A high-speed Photron SA-Z high-speed camera was used in concert with a 45° mirror, 5x magnification microscope objective, and a tube lens to record the visible images from the scintillator at frame rates from 20 to 90 kHz. Specifically, the achieved frame rates for each presented sample were: S1 (90 kHz), S2 (80 kHz), S3 (70 kHz), and M1 (20 kHz). The beam was operated in concert with a set of mechanical shutters in order to limit the total time of on-sample radiation to prevent sample and scintillator damage, and therefore the beam was only unblocked for approximately 12.5 ms every 1 s. Accordingly, a burst of images was taken of the sample under constant mechanical excitation every 1 s. Due to this restriction, the majority of the duration for which the sample was subjected to mechanical excitation was not captured. A schematic of this experimental setup is shown in Fig. 2.

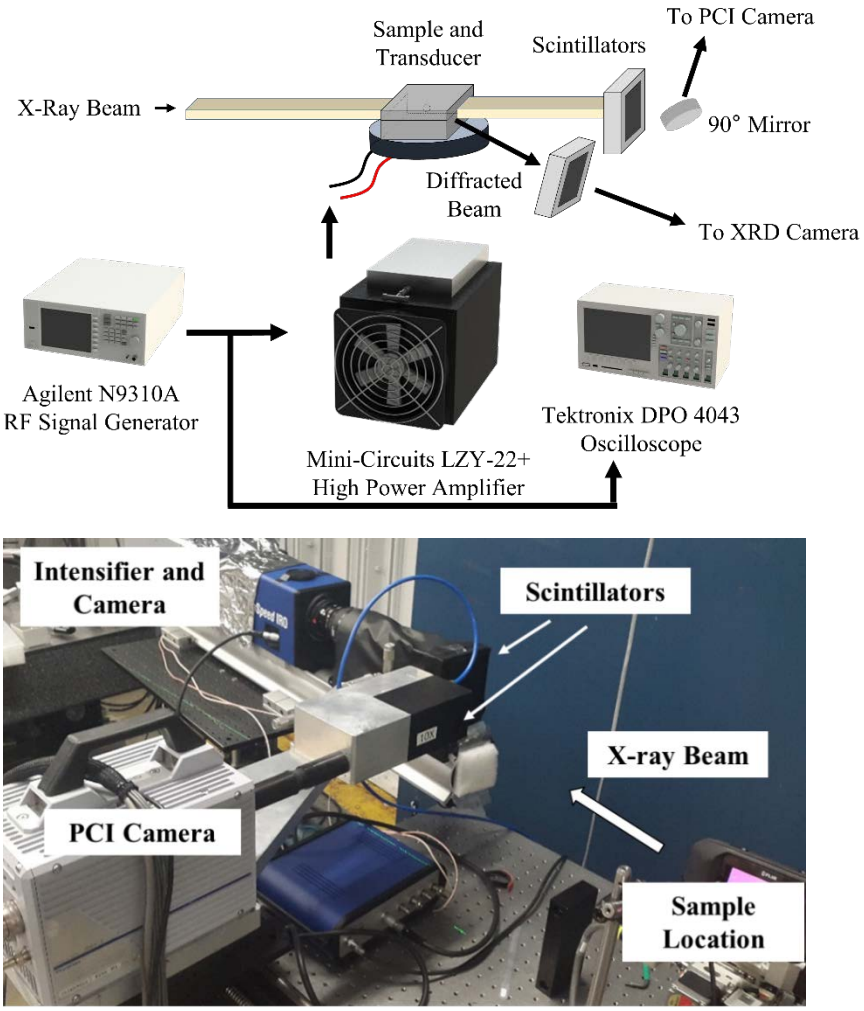

Figure 2. A diagram of the X-ray phase contrast imaging and diffraction setup of the ultrasonically excited sample and a photograph of the setup at the 32-ID-B hutch.

A high-speed Photron SA-Z camera with a Lavision HS-IRO image intensifier with a gating time of 200 ns and a gain of 70% was used to image a $Lu_3Al_5O_{12}$:Ce scintillator offset from the X-ray beam axis to image the diffraction peaks from an aluminum calibration sample and the sample M2, containing three contacting HMX particles. The observed angular range was $2\theta = 8 - 15°$ degrees with a resolution of 0.013°. The diffraction data was collected in transmission mode at 20 kHz for burst durations of 12.5 ms at each 1 s interval over 10 s. The nominal X-ray wavelength was 0.51176 Å. The sample was mounted on a rotating stage and the angle was adjusted until a diffraction peak appeared, which was determined to correspond to the (-2 3 1) plane. HiSPoD software [17] was used to analyze the diffraction patterns to obtain time dependent peak shifts and lattice spacing. The peak shifts were used to infer the temperature changes using the thermal expansion coefficients for the β-HMX crystals. This method achieved a temperature resolution of ~12 K resulting from the resolution of the measured X-ray diffraction peak (0.013º). The thermal expansion coefficients were calculated using the raw data in [16] for

the lattice planes (1 -2 0), (0 1 1), (-1 2 2) and (0 3 1) with the lattice parameters of a = 6.537 Å, b = 11.054 Å, c = 8.7018 Å and β = 124.443° (JCPDS listing 42-1768). The amounts of expansion percentages for these planes for a temperature change from 30° to 150°C were measured as 1.394%, 1.097%, 0.797% and 1.617% respectively. For a monoclinic crystal, the lattice spacing d corresponding to a set of Miller indices (h, k, l) can be calculated using the following equation:

$$\frac{1}{d^2} = \frac{1}{\sin(\beta)^2}\left(\frac{h^2}{a^2} + \frac{k^2\sin(\beta)^2}{b^2} + \frac{l^2}{c^2} - \frac{2hl\cos(\beta)}{ac}\right)$$

The 4 unknown lattice thermal expansion coefficients (α_a, α_b, α_c, α_β) for the monoclinic crystal were calculated as 6.471×10^{-5}, 1.509×10^{-4}, 4.872×10^{-5} and -3.388×10^{-5} K^{-1} respectively. Using these values, the coefficient of thermal expansion for the (-2 3 1) plane was calculated as 1.126×10^{-4} K^{-1}, which was used to determine temperature rise for the sample.

In an attempt to verify the estimated temperatures of the crystal, the inferred temperature history of the particle was used to simulate the temperature evolution at the sample surface using a commercial finite element package. The measured temperature was used as a boundary condition applied at a planar disk with a diameter the nominal size of the particles, 500 µm, at a depth of 1 mm under the surface of a Sylgard 184 sample domain with identical dimensions as the original samples of 6.6 x 9.0 x 4.0 mm. The thermal conductivity, density, and heat capacity used were 0.232 W/m-K, 1030 kg/m^3, and 1630 J/kg-K, respectively. The results were compared to a previous study that measured the surface temperatures of a similar sample using infrared imaging [21].

3. Results

In order to reduce the number of potential mechanical interactions which may occur within a fully dense composite explosive system, a simplified model system consisting of a single particle fully embedded within an elastic binder matrix was investigated. Samples were constructed of Sylgard 184 binder material with a single embedded HMX explosive particle with a particle size ranging from 500 µm up to 2 mm. This simplified model system eliminated the effects of the numerous particle-particle interactions present in fully dense composite materials, and allowed for the investigation of the potential mechanisms active for a single particle-binder system. Such mechanisms of interest would include viscoelastic wave scattering effects, plastic deformation of the surrounding binder material, and the dynamic interactions occurring at the particle-binder interface, as suggested in prior studies [3-6]. High-frequency mechanical excitation was generated and transferred into the binder material via a ceramic ultrasonic transducer attached to the sample surface with epoxy as shown in Fig. 3. The transducer was driven via a sinusoidal electrical signal of 10 W at a fixed frequency of 210 kHz for a continuous excitation time of 10 s, as presented for a similar experimental setup in previous work [3, 6, 7].

This experiment was conducted at beam line 32-ID-B at APS at ANL which allowed for high-resolution X-ray phase contrast images of the ultrasonically driven energetic particle within the binder material. The dynamic response of the HMX particle and surrounding binder to the applied mechanical excitation was imaged at selected framerates of 20-90 kHz for a continuous duration up to 12.5 ms. The effective burst of high-speed imaging was then repeated throughout the duration of the experiment at 1 s intervals. The X-ray irradiation of the sample was synchronized with the image recording, which was performed in order to limit damage to the sample and instrumentation. A representative frame achieved via the HS-XPCI of an HMX particle and surrounding binder is shown in detail in Fig. 4.

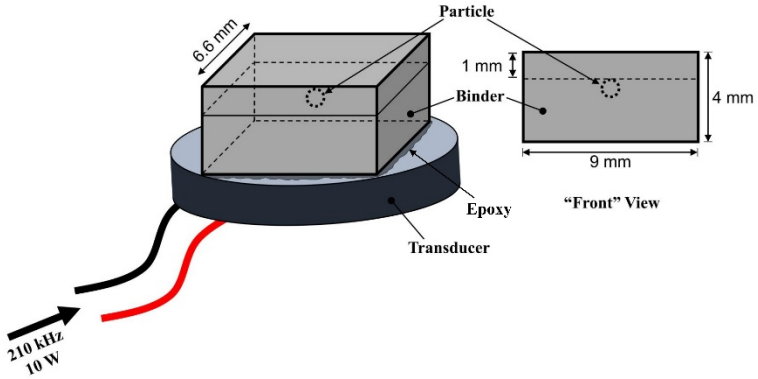

Figure 3. A diagram of the sample construction and application of the high-frequency mechanical excitation.

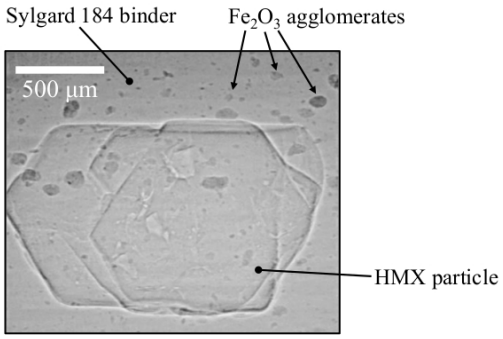

Figure 4. An X-ray phase contrast image of the HMX particle within Sylgard 184 binder. Fe_2O_3 powder was added to the binder material to increase contrast. Some Fe_2O_3 powder resulted in large agglomerates appearing present in the sample as highlighted.

A total of five samples consisting of a single embedded HMX particle were investigated via the aforementioned technique. Results obtained from two of the samples are presented here in detail to illustrate the dynamic response of the embedded particles as observed via this technique. Selected frames from the HS-XPCI of the sample referenced as S1 are presented in Fig. 5. For sample S1, the HMX particle and surrounding binder material exhibited no significant dynamic response to the applied high-frequency mechanical excitation during the first 8 s of the trial. However, the particle shifted upward throughout the experiment and this effect is clearly

presented in frames (a) through (c) of Fig. 5. This effect was attributed to the bulk heating and subsequent thermal expansion of the binder material in response to either the high-frequency mechanical excitation or X-ray radiation, although the mechanical support of the sample may have shifted during the trial. After a duration of 8 s, the HMX particle experienced slight cracking, mainly in the center region of the particle as observed in frame (d). Additionally, a distinct cyclic motion occurring at the particle-binder interface was observed at the bottom right of the particle boundary, and at regions where significant cracking of the particle occurred. The cracking of the particle appeared to extend throughout the particle and this effect is clearly visible in frames (d) and (e). The cyclic motion of the binder continued until the end of mechanical excitation at 10 s. Delamination of the binder material from the embedded HMX particle occurred after 7 to 8 s of high-frequency mechanical excitation. This result demonstrates that relatively weak high-frequency mechanical excitation can force debonding of the binder material from an embedded HMX particle. The initial delamination appeared to be amplified by the applied mechanical excitation and the defect advanced along the particle-binder interface. The dynamic motion at the interface, along with the heating supplied to the particle via the mechanical excitation appeared to induce the observed cracking of the embedded HMX particle.

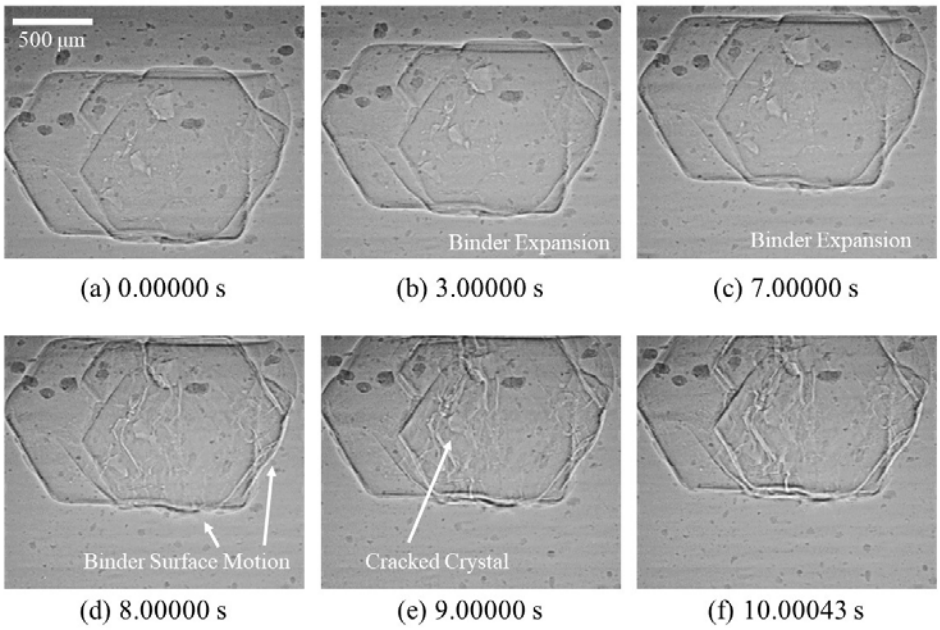

Figure 5. Select frames of the X-ray phase contrast imaging of Sample S1 under ultrasonic excitation (access video here).

A selection of frames from the HS-XPCI of the sample referenced as S2 in response to the applied high-frequency mechanical excitation is presented in Fig. 6. The immediate response of the sample to the applied mechanical excitation exhibited evidence that a delaminated area was initially present at the bottom right position on the particle-binder interface; this location is marked in frame (a). A distinct cyclic motion, similar to that observed in sample S1, was immediately evident over a small region on the particle-binder interface as the mechanical excitation was initially applied to the sample. This result suggests that a defect was generated

either at the time of fabrication or through handling during the transportation or set-up of the sample for the experiment. As the mechanical excitation continued, the delamination was observed to spread along the particle boundary to the right and bottom sides of the particle and eventually encompassed the entire particle at a duration of 8 s. The cyclic motion of the binder material along the particle interface occurred where the delamination was present. This process is presented in frames (a) through (e) in Fig. 6. During the delamination process, significant cracking of the particle was observed near the initial debond region and spread throughout the particle, likely due to the β to δ phase change of HMX at elevated temperatures [16, 18]. At 8 s of excitation, a region of the embedded particle had transitioned into a HMX melt, which underwent observable gasification, as highlighted in frame (d). At a duration of 9 s, the particle boundary underwent a significant expansion in size, which was likely due to the further gasification of the HMX melt and pressure build-up. The expansion event of the boundary is clearly shown between frames (e) and (f). A major portion of the energetic particle was observed to transition into an HMX melt in frames (e) through (g), while the gasification intensified until the binder material surrounding the particle ruptured (h), at which point all observable dynamic motion ceased. The observed response of this sample indicates that an initial delamination defect, present at a localized region along the particle-binder interface, can be advanced along the particle surface by the applied high-frequency mechanical excitation. The cyclic motions at the particle-binder interface appeared to drive cracking, phase change, and gasification of the HMX particle within the sample via a contact friction heating mechanism. The melt and gasification of the HMX particle are clear indications of the decomposition of the explosive particle [19, 20] in response to the applied mechanical excitation.

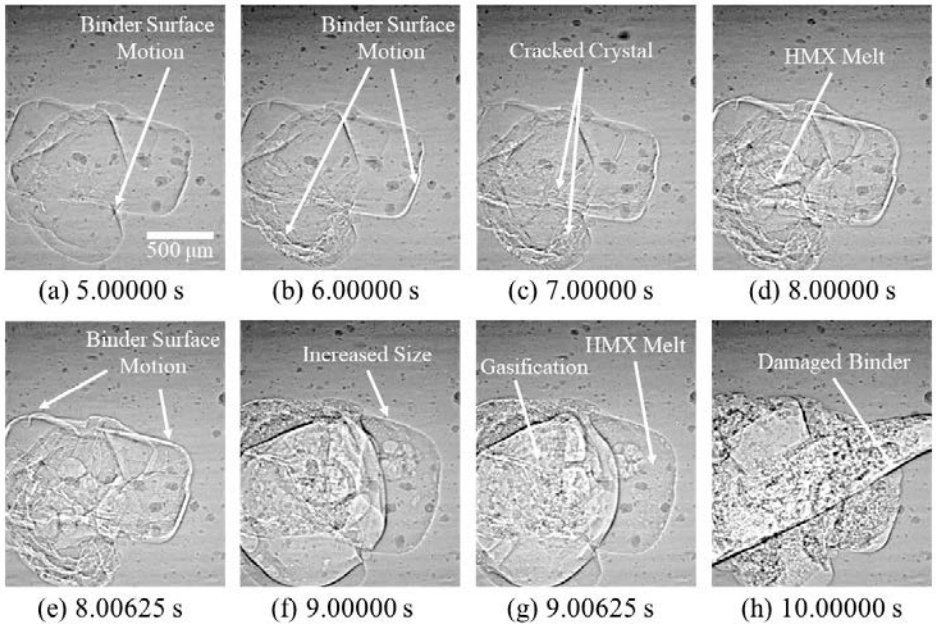

Figure 6. Select frames of the X-ray phase contrast imaging of Sample S2 under ultrasonic excitation (access video here).

A similar response was also observed from an additional sample (S3) such that significant cyclic motion of the binder material at the interface appeared to drive the particle to heat and fracture. After a duration of 5 s of excitation, the entire particle then appeared to transition into an HMX melt and rapid gasification of the energetic material was observed to occur. After a duration of 6 s of mechanical excitation, the binder material surrounding the HMX particle ruptured and all observable motion ceased. The HS-XPCI of the responses of the S2 and S3 samples clearly demonstrates the ability of high-frequency mechanical excitation to drive significant motion at a delamination defect at the particle-binder interface. The thermal response and dynamic motion occurring at the defect was then able to drive further delamination along the interface, and enabled the decomposition of the energetic material resulting in mechanical failure and rupture of the surrounding binder.

The results of the final two additional samples embedded with a single HMX particle showed significant cracking of the particle; however, neither of the energetic particles appeared to undergo a similar degree of decomposition that was observed in samples S2 and S3 within the same time frame.

In order to evaluate the effects of the X-ray radiation on the samples, two additional samples were imaged up to an extended duration of 20 s using the identical imaging conditions of the previously reported samples with no applied ultrasonic excitation. The binder material was observed to notably expand, likely due to thermal expansion; however, no significant damage or physicochemical change was observed within the HMX particles. In one sample, a localized delamination of the particle-binder interface was noted. This delamination appeared to only affect a small region along the particle-binder interface. Therefore, it was concluded that the direct effect of the X-ray radiation was minimal, but not entirely negligible.

The HS-XR PCI technique allowed for clear observation of the dynamic response of the single particle and binder system to the applied mechanical excitation. This process was therefore extended to investigate the response of samples containing a relatively low-density single layer of explosive particles to an ultrasonic insult. Additional samples, similar to the simplified single particle models, were constructed such that HMX particles were positioned in a single plane fully embedded within the binder material. The plane of the explosive particles was orthogonal to the incident ultrasonic insult, and was along the viewing axis of the HS-XR PCI. Two samples of this configuration were mechanically excited and observed using the same experimental procedure adopted for the single particle systems. Select frames of the HS-XR PCI of one of the additional multi-particle samples, M1, in response to the applied high-frequency mechanical excitation is presented in Fig. 7.

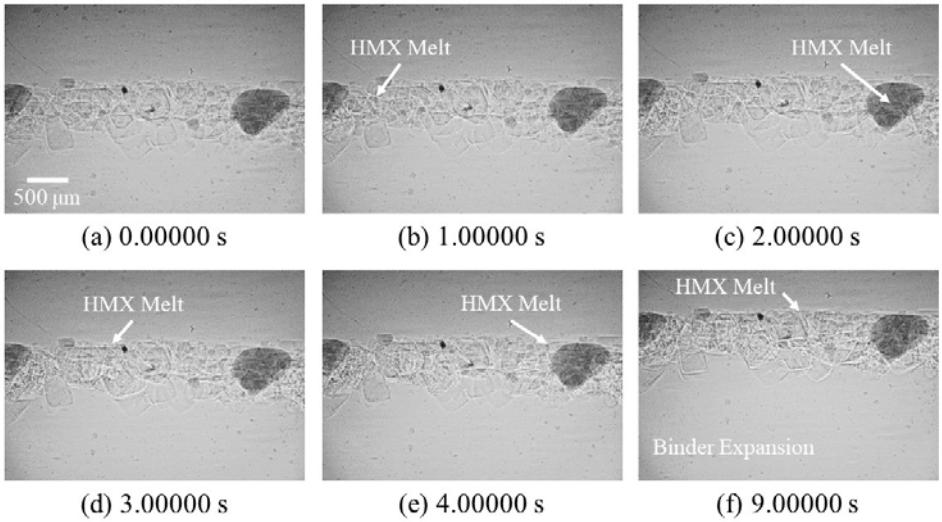

Figure 7. Select frames of the X-ray phase contrast imaging of sample M1 under ultrasonic excitation (access video here).

Throughout the application of ultrasonic excitation to the sample, various regions of HMX particles exhibited evidence of the formation of HMX melt and gasification at various durations of the mechanical excitation. At each of these locations, which are highlighted in frames (b) through (f), the formation of HMX melt and gasification was evident across an apparent spatial region of approximately 500 µm. In almost all of these cases, these regions had quenched in the next burst of captured images; however, other locations were undergoing a transition to an HMX melt which progressed to observable gasification. This process of HMX melt/gasification and subsequent quenching occurred at multiple localized regions until the application of the ultrasonic excitation to the sample was interrupted. A similar response to the high-frequency mechanical excitation was also observed in the second multiple particle sample. Due to the configuration of the experiment, with the view in-line with the plane of particles, it was difficult to inspect the dynamic response of the multiple HMX particles for specific particle-particle interactions.

After ultrasonic excitation and HS-XR PCI of the samples were performed, each sample was inspected via optical microscopy; images of samples S2 and M1 are presented in Fig. 8. As shown in Fig. 8(a), a large portion of the single HMX particle underwent significant chemical decomposition. A small portion of the embedded particle still appears as a solid form of the original HMX particle; however, the opaque residue around the remaining particle appears to be condensed product or a solidification of the HMX melt, which would likely exist as δ phase. It is also clear that the gasification of the embedded HMX particle was able to significantly expand the surrounding binder creating a noticeable void around the particle and residue of the HMX particle. The multiple particle sample, M1, presented in Fig. 8(b), shows a clear pattern of opaque HMX particles near the center of the sample indicating the focal region of the ultrasonic excitation supplied by the transducer. The increased opacity of the energetic particles is attributed to either the partial decomposition of the particle or to the β to δ phase change of the HMX incurred via a thermal rise of the particle. This phase change results in the rearrangement

of the particle structure which subsequently shatters due to the volumetric increase of the particle [16, 18], causing the HMX to become opaque and white due to increased light scattering [7, 21]. It is clear that the ultrasonic excitation induced a significant response in multiple HMX particles within an approximate diameter of effect of 5.1 mm in this experimental configuration.

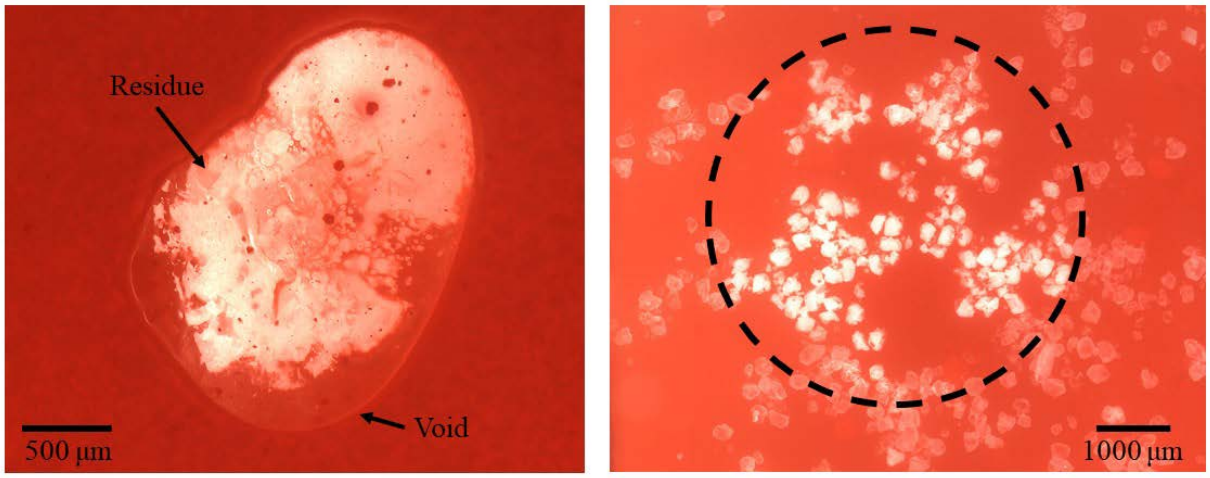

(a) (b)

Figure 8. (a) An optical microscopy image of the partially decomposed HMX particle within a Sylgard 184 binder of sample S2 after the application of ultrasonic excitation. (b) An optical microscopy image of multiple HMX particles within a Sylgard 184 binder of sample M1 after the application of ultrasonic excitation. The ultrasonically affected area demonstrated by the opaque HMX particles is highlighted.

Simultaneous HS-XPCI and HS-XRD were also performed during the excitation of an additional sample M2. This sample contained three β-HMX particles in contact at the center of the sample, positioned in an equilateral triangle pattern, similar to samples reported in Roberts et al. [22]. The transducer for this sample was permanently attached to a substrate to prevent sample motion. Visible degradation, delamination, expansion of the particles, and the absence of decomposition were similar to the observations of sample S1. Fig. 9 shows the phase contrast image of the sample and the corresponding XRD spot from the (-2 3 1) crystal plane from one of the particles, overlaid with lattice spacing contours. The broadness of the diffraction spot was due to the X-ray energy spectrum, as shown in Fig. 1. As the sample was held under ultrasonic excitation, the diffraction peak of interest shifted to lower angles as the crystal expanded, as illustrated in Fig. 10(a). The progression of this XRD peak shift was nearly linear with time and reached a value of 0.2° after 10 s. This shift in the XRD peak was used as a measure of the expansion of the crystal lattice over time. With the values of the coefficient of thermal expansion of the β-HMX calculated using the data in [16], the measured lattice expansion was used to infer the transient temperature of the particle. The corresponding transient temperature of the particle is shown in Fig. 10(b) with a maximum temperature rise of ~180 K in 10 s.

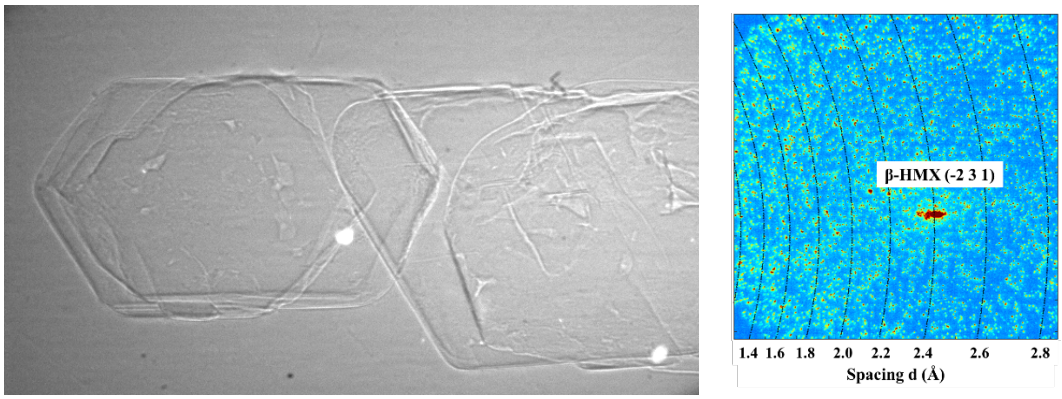

(a) (b)

Figure 9. (a) An X-ray phase contrast image of the three crystals embedded in the Sylgard 184 binder and (b) the simultaneous X-ray diffraction peak from the lattice plane of (-2 3 1) from one of the crystals overlaid with lattice spacings.

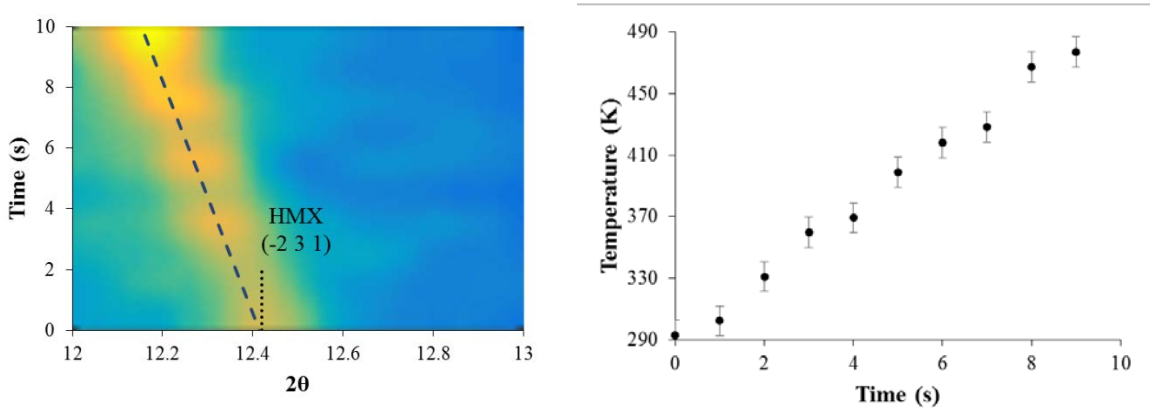

(a) (b)

Figure 10. (a) The X-ray diffraction peak shift of a β-HMX particle due to thermal expansion measured at a rate of 20 kHz and (b) the corresponding temperature rise calculated using the thermal expansion coefficient at each second.

The results indicate that the sample reached a temperature of ~470 K in 10 s. The linearity of the temperature rise indicates heating due to a near-constant flux heat source. This sample did not show a phase change or decomposition event as the β to δ-HMX polymorphic transformation takes nearly 400 s at this temperature [23]. For additional verification of the temperature estimation of the particle, a finite element simulation was conducted to model the temperature of the Sylgard 184 sample surface due to heating from an embedded planar disk of an area corresponding to the particle size, following the temperature history presented in Fig. 10. The modeled surface temperature, shown in Fig. 11(a) compares well with previously measured surface temperatures of a similar sample under identical mechanical excitation conditions as reported in Roberts et al. [22]. The predicted maximum temperature rise is 8 K within 4 s, which is within the range of reported sample surface temperatures [22]. The spatial thermal profile presented in Fig. 11(b) is also comparable to those reported [22].

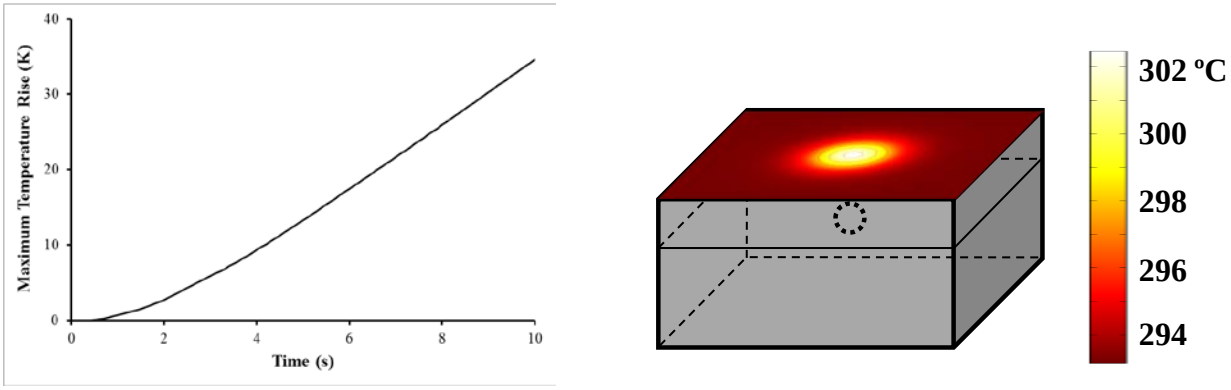

(a) (b)

Figure 11. (a) The predicted maximum surface temperature rise on the surface of the sample as a function of time using the measured particle temperature in Fig. 10(b) and (b) spatial distribution of the surface temperature after 4 s.

4. Discussion

The results obtained from the HS-XR PCI clearly demonstrate the ability of high-frequency mechanical excitation to create significant mechanical damage along the particle-binder interface, generate a thermal response from the embedded particle, and induce significant chemical decomposition of the energetic material. The observed response of sample S1 to the applied mechanical insult demonstrates that a debond between the particle and the surrounding binder was forced at a localized region at the incident side of the embedded HMX particle. Previous work [5], found that significant stress concentrations may occur within a viscoelastic material near an embedded spherical inclusion under plane-wave acoustic excitation. Specifically, the authors utilized an analytical model similar to the sample configuration and the mechanical excitation used in this work to show that significant localized heating near the incident side of the inclusion can occur due to wave interaction effects within a viscoelastic material. The energy localization observed in that model was due to the interaction of the scattered waves near the impedance mismatch of the particle-binder interface. It was suggested that the localized heating would induce a significant thermal expansion of the binder material near the particle surface and that this effect over time, along with the dynamic stresses occurring at the particle-binder interface, could debond the binder material from the particle surface. Therefore, it is expected that the thermal expansion of the binder material near the incident side of the particle, in concert with the dynamic stresses at the interface, induced via the applied high-frequency mechanical excitation led to the delamination observed in sample S1.

Furthermore, the applied excitation was able to drive significant cyclic motion at the defect site which appeared to advance the delamination along the particle-binder interface. This cyclic motion of the binder material at the particle surface is likely to generate heat at this location through a “rubbing” or “slapping” frictional mechanism [24]. This generation of localized heating would lead to a significant temperature rise of the binder material as well as the embedded HMX particle over time. The particle was also observed to crack after a duration of 8

s of mechanical excitation. This cracking may be associated with the aforementioned β to δ phase change of the HMX material which begins to occur near a temperature of 433 K [20]. This explanation of the cracking of the particle due to a thermally induced phase change is strengthened by the observed whitening of the embedded HMX particles in sample M1 after the applied mechanical excitation, as shown in Fig. 8(b).

The observed responses of samples S2 and S3 illustrate that cyclic motion at locations of delamination yielded a significant thermal response of the embedded energetic particles. The generated thermal energy from this process was sufficient to induce not only a β to δ phase transition, but also a significant decomposition of much of the HMX particle as signaled by a visible melt phase accompanied with gasification. These results clearly demonstrate that a significant portion of the HMX material was driven to chemical decomposition through various heating mechanisms induced by the applied mechanical excitation. It should be noted that an additional heat generation mechanism resulting from the chemical decomposition of the HMX material would yield additional thermal energy to the system, which, in turn, could assist in driving the continued decomposition of the energetic material. This ability to drive HMX particles to decomposition by applied high-frequency mechanical excitation was also demonstrated in samples containing a low-density single layer of particles. In those samples, it was observed that multiple locations of HMX melt and gasification were present at different times throughout the duration of the applied mechanical excitation.

The observation from simultaneous HS-XPCI and HS-XRD on the sample M2 demonstrates that the diffraction peak shift from an embedded HMX crystal heated under ultrasonic excitation can be used to infer the temperature history of the particle. This method enables sub-surface temperature measurements and can be a valuable tool for other systems. Furthermore, this method may be extended to allow for faster measurement rates, which are limited by the intensifier gating time and camera limitations.

5. Conclusions

The combination of these results suggests that the ultrasonically driven decomposition of embedded HMX particles within a viscoelastic binder material may occur through the procession and build-up of three primary heating mechanisms. The initial heating of the region near the embedded particle is likely caused by the viscoelastic dissipation of the periodic stress concentrations developed near the incident side of the particle due to the previously explored [5] wave-scattering effect. Due to the combination of the thermal expansion of the binder material and the dynamic stresses along the particle-binder interface, the binder can then become debonded from the particle, allowing for a frictional heating mechanism via the cyclic motion at the forced defect driven by the applied mechanical excitation. Local regions of the HMX particle are then thermally driven to chemical decomposition, which allowed for the final additional heat generation mechanism.

It is expected that the debonding of the binder material from the particle surface due to the thermal expansion and dynamic stresses of the binder is critical in order for an additional frictional mechanism to occur. As such, it is expected that the thermal expansion behavior and the adhesion between the energetic material and binder materials are of extreme importance in

order to either suppress or possibly exploit this phenomenon of ultrasonically driven decomposition.

Data Availability

The raw/processed data required to reproduce these findings cannot be shared at this time as the data also forms part of an ongoing study.

Acknowledgements

This research is supported by the U.S. Office of Naval Research [grant number N00014-11-1-0466]; by the U.S. Air Force Office of Scientific Research [award numbers FA9550-15-1-0102, FA9550-15-1-0202]; and by the National Science Foundation Graduate Research Fellowship Program [grant number DGE-1333468]. This research used resources of the Advanced Photon Source, a U.S. Department of Energy (DOE) Office of Science User Facility operated for the DOE Office of Science by Argonne National Laboratory under contract number DE-AC02-06CH11357. The authors would also like to acknowledge the assistance of Alex Deriy and Jin Wang at APS, and Matthew Beason and Tugba Isik for their help with experiments.

References

[1] M.W. Chen, S. You, K. S. Suslick, and D. D. Dlott, "Hot spots in energetic materials generated by infrared and ultrasound, detected by thermal imaging microscopy," *Rev. Sci. Instrum.* 85 (2014) 023705.

[2] S. You, M.W. Chen, D. D. Dlott, and K. S. Suslick, "Ultrasonic hammer produces hot spots in solids," *Nat. Commun.* 6 (2015) 6581.

[3] J. O. Mares, J. K. Miller, I. E. Gunduz, J. F. Rhoads, and S. F. Son, "Heat generation in an elastic binder system with embedded discrete energetic particles due to high-frequency, periodic mechanical excitation," *J. Appl. Phys.* 116 (2014) 204902.

[4] J. O. Mares, J. K. Miller, N. D. Sharp, D. S. Moore, D. E. Adams, L. J. Groven, J. F. Rhoads, and S. F. Son, "Thermal and mechanical response of PBX 9501 under contact excitation," *J. Appl. Phys.* 113 (2013) 084904.

[5] J. O. Mares, D. C. Woods, C. E. Baker, S. F. Son, J. F. Rhoads, J. S. Bolton, and M. Gonzalez, "Localized heating near a rigid spherical inclusion in a viscoelastic binder material under compressional plane wave excitation," *J. Appl. Mech.* 84 (2017) 041001.

[6] J. K. Miller, J. O. Mares, I. E. Gunduz, S. F. Son, and J. F. Rhoads, "The impact of crystal morphology on the thermal responses of ultrasonically-excited energetic materials," *J. Appl. Phys.* 119 (2016) 024903.

[7] Z. A. Roberts, J. O. Mares, J. K. Miller, I. E. Gunduz, S. F. Son, and J. F. Rhoads, "Phase changes in embedded HMX in response to periodic mechanical excitation," in: B. Antoun, A. Arzoumanidis, H. J. Qi, M. Silberstein, A. Amirkhizi, J. Furmanski, and H. Lu (Eds.), *Challenges in Mechanics of Time Dependent Materials, Volume 2*, Springer, 2017, pp. 79-86.

[8] J. E. Field, N. K. Bourne, S. J. P. Palmer, S. M. Walley, J. Sharma, and B. C. Beard, "Hot-spot ignition mechanisms for explosives and propellants [and discussion]," *Philos. Trans.: Phys. Sci. Eng.* 339 (1992) 269-283.

[9] D. S. Moore, "Instrumentation for trace detection of high explosives," *Rev. Sci. Instrum.* 75 (2004) 2499-2512.
[10] D. S. Moore, "Recent advances in trace explosives detection instrumentation," *Sens. Imaging: Int. J.* 8 (2007) 9-38.
[11] H. Ostmark, S. Wallin, and H. Ang, "Vapor pressure of explosives: a critical review," *Propell., Explos., Pyrot.* 37 (2012) 12-23.
[12] National Research Council (U.S.). Committee on the Review of Existing and Potential Standoff Explosives Detection Techniques., *Existing and potential standoff explosives detection techniques*. Washington, D.C.: National Academies Press, 2004.
[13] N. P. Loginov, "Criteria for estimation of explosion hazard in producing and processing explosives under vibration," *Combust., Expl., Shock*+ 36 (2000) 633-638.
[14] N. P. Loginov, "Decomposition of lead azide, pentaerythrite tetranitrate, and a laminate system composed of these substances under vibrational loading," *Combust., Expl. Shock* 45 (2009) 64-69.
[15] F. P. Bowden and A. D. Yoffe, *Initiation and growth of explosion in liquids and solids*. New York: Cambridge University Press, 1985.
[16] C. K. Saw, "Kinetics of HMX and phase transitions: effects of grain size at elevated temperature," *12th International Detonation Symposium*, San Diego, CA, August 11-16, 2002.
[17] T. Sun and K. Fezzaa, "HiSPoD: a program for high-speed polychromatic X-ray diffraction experiments and data analysis on polycrystalline samples," *J. Synchrotron Radiat.* 23 (2016) 1046-1053.
[18] C. Xue, J. Sun, B. Kang, Y. Liu, X. Liu, G. Song, and Q. Xue, "The β-δ-phase transition and thermal expansion of octahydro-1, 3, 5, 7-tetranitro-1, 3, 5, 7-tetrazocine," *Propell., Explos., Pyrot.* 35 (2010) 333-338.
[19] R. Karpowicz and T. Brill, "In situ characterization of the “melt” phase of RDX and HMX by rapid-scan FTIR spectroscopy," *Combust. Flame* 56 (1984) 317-325.
[20] N. Kubota and S. Sakamoto, "Combustion mechanism of HMX," *Propell., Explos., Pyrot.* 14 (1989) 6-11.
[21] L. Smilowitz, B. Henson, B. Asay, and P. Dickson, "The β–δ phase transition in the energetic nitramine-octahydro-1, 3, 5, 7-tetranitro-1, 3, 5, 7-tetrazocine: Kinetics," *J. Chem. Phys.*, vol. 117, pp. 3789-3798, 2002.
[22] Z. A. Roberts, A. D. Casey, I. E. Gunduz, J. F. Rhoads, and S. F. Son, "The effects of crystal proximity and crystal-binder adhesion on the thermal responses of ultrasonically-excited composite energetic materials," *J. Appl. Phys.* 122 (2017) 244901.
[23] B. Henson, L. Smilowitz, B. Asay, and P. Dickson, "The β–δ phase transition in the energetic nitramine octahydro-1, 3, 5, 7-tetranitro-1, 3, 5, 7-tetrazocine: thermodynamics," *J. Chem. Phys.* 117 (2002) 3780-3788.
[24] M. Rothenfusser and C. Homma, "Acoustic thermography: vibrational modes of cracks and the mechanism of heat generation," *AIP Conf. Proc.* 760 (2005) 624-631.